

# SAW Sensors Using Orthogonal Frequency Coding

D. Puccio<sup>1</sup>, D. C. Malocha<sup>1</sup>, D. Gallagher<sup>1</sup>, and J. Hines<sup>2</sup>

<sup>1</sup>Electrical and Computer Engineering Department, University of Central Florida, Orlando, FL 32816-2450

<sup>2</sup>Microsensor Systems, Inc., Bowling Green, KY

**Abstract-** The SAW sensor offers advantages in that it is wireless, passive, small and has varying embodiments for different sensor applications. In addition, there are a variety of ways of encoding the sensed data information for retrieval. Single sensor systems can typically use a single carrier frequency and a simple device embodiment, since tagging is not required. In a multi-sensor environment, it is necessary to both identify the sensor as well as obtain the sensed information. The SAW sensor then becomes both a sensor and a tag. For multi-sensor systems, many embodiments use coded reflectors having a single carrier frequency. In previous work, several authors have shown that there are advantages of using spread spectrum techniques for device interrogation and coding, such as enhanced processing gain and greater interrogation power.

This paper will present a spread spectrum approach using orthogonal frequency coding (OFC) for encoding the SAW sensor. The encoding technique is similar to M-ary FSK in terms of its implementation where a transducer or reflector is built with the desired code. It is shown that the time ambiguity in the autocorrelation due to the OFC is significantly reduced as compared to a single frequency tag having the same code length. The OFC approach is general and should be applicable to many differing SAW sensors for temperature, pressure, liquids, gases, etc. Device embodiments are shown, and a discussion is provided for device design considerations such as the number of chips used, chip length, transducer fractional bandwidth, and chosen piezoelectric material. Measured device results are presented and compared with COM model predictions to demonstrate performance. Devices are then used in computer simulations of multiple transceiver designs and the results are discussed.

## I. INTRODUCTION

SAW sensors have been widely studied and offer many advantages including wireless, passive operation and the ability to operate in harsh environments. SAW sensors are capable of measuring physical, chemical and biological variables [1,2]. Current embodiments include delay line and resonator-based oscillators, differential delay lines, and devices utilizing multiple reflective structures. However, few SAW sensor embodiments are capable of operation in multi-sensor environments [3]. In multi-sensor systems, the sensor must transmit identification and sensor information simultaneously. This paper demonstrates a spread spectrum approach using orthogonal frequency coding (OFC) for coding SAW sensors. Since OFC coding is a spread spectrum technique, it has the inherent advantage of processing gain, security, CDMA, and spectrum spreading. In addition, OFC coded systems are capable of meeting the ultra-wide band (UWB) specifications. In this paper, SAW device embodiments for ID tags and sensors are described.

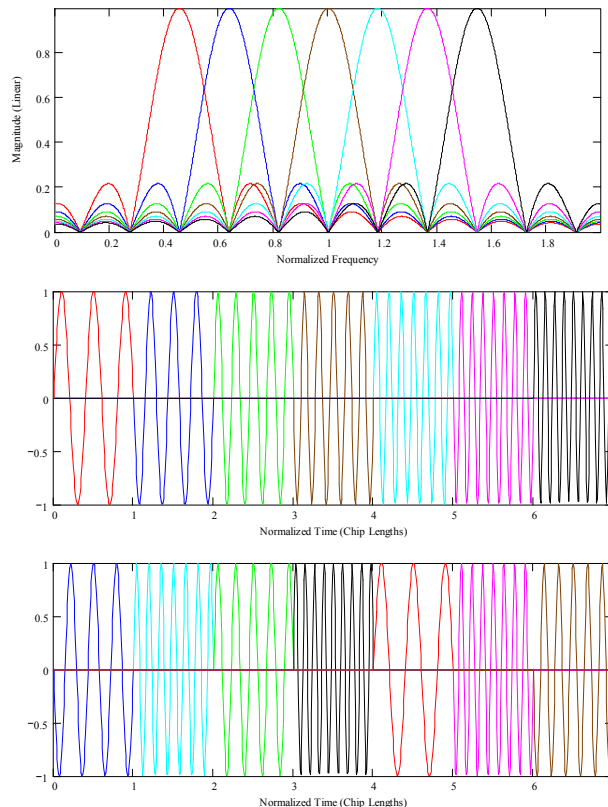


Figure 1. Example of OFC chip frequency responses (upper), stepped chirp response (middle), orthogonal frequency coded waveform (lower)

Devices are simulated and compared with experimental results on YZ LiNbO<sub>3</sub>.

## II. ORTHOGONAL FREQUENCY CODING

Orthogonal frequency coding (OFC) is similar to M-ary FSK [4]. Orthogonal frequencies are used to spread the signal bandwidth. The orthogonality condition describes a relationship between the local chip frequencies and their bandwidths. As an example, consider the stepped linear chirp shown in Fig. 1 [5]. Seven coherent carriers are used to generate the signal shown. Each chip contains an integer number of carrier half cycles due to the orthogonality condition. Under these conditions, the resulting waveform is continuous. Also note the chip frequency responses in Fig. 1. These responses are a series of sampling functions with null bandwidths equal to  $2\tau^{-1}$ . In addition, the sampling function center frequencies are separated by multiples of  $\tau^{-1}$ . Coding is

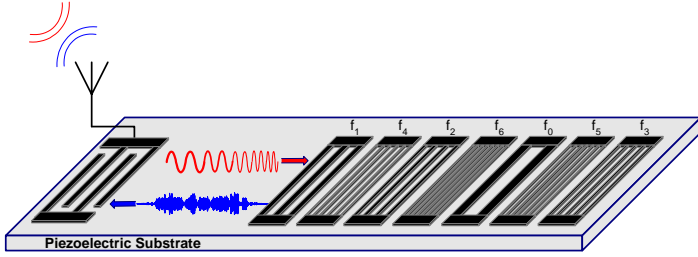


Figure 2. Schematic drawing of seven chip OFC SAW ID tag. Grating periodicities are chosen so that grating center frequencies match the chip carrier frequencies. Interrogation signal (red) is stepped linear chirp and returned signal (blue) is noise-like.

accomplished by shuffling the chips shown in the stepped chirp signal as shown in Fig. 1. The code is now determined by the order in which the orthogonal frequencies are used. Both signals occupy the same bandwidth and the coded information is contained within the signal phase. A more complete description of orthogonal frequency coding is given by Malocha, et al [6].

### III. OFC SAW ID TAG IMPLEMENTATION

OFC waveforms can be employed in SAW devices using shorted periodic reflector gratings as shown in Fig. 2. Each chip of the OFC waveform is implemented using a shorted periodic reflector grating. The grating periodicities are chosen so that the grating center frequencies correspond to the chip carrier frequencies. In order to keep the chip length approximately constant, each grating must contain different numbers of electrodes as the periodicity changes. This is a direct result of the orthogonality condition. The equation used to find the grating electrode counts is shown below.

$$N_j = \tau_c \cdot f_j \quad (1)$$

This equation shows that the grating electrode count is directly proportional to frequency. In addition, the normalized metal

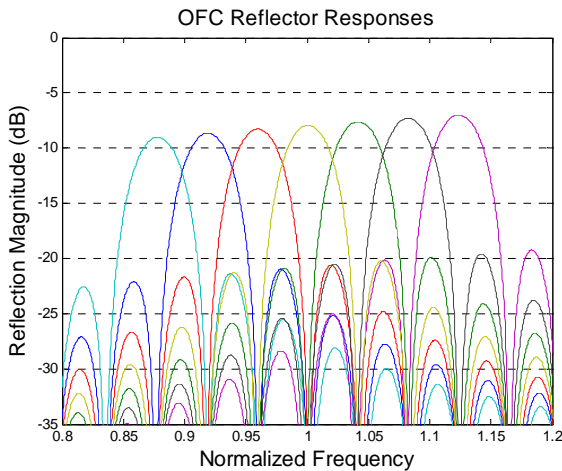


Figure 3. Shorted reflector grating responses for seven chip OFC SAW tag

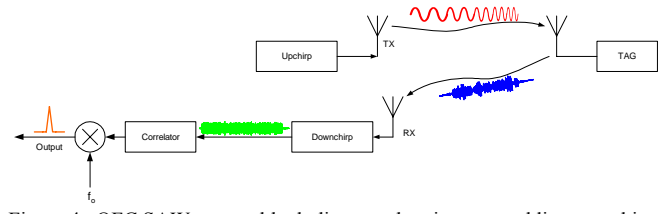


Figure 4. OFC SAW system block diagram showing stepped linear upchirp interrogation (red) and returned noise-like signal (blue). Compressed pulse results after application of downchirp and matched filtering.

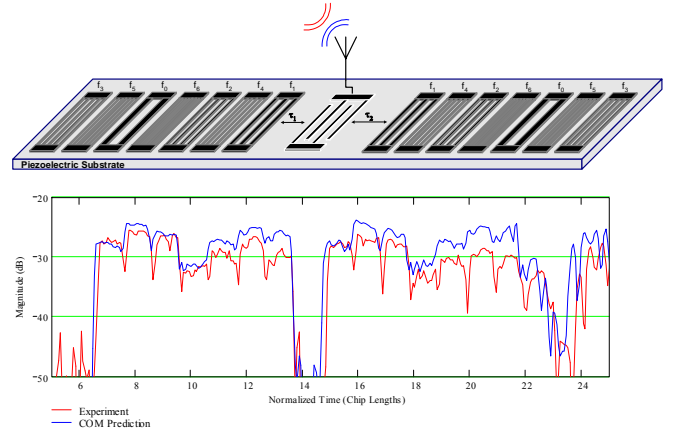


Figure 5. OFC SAW sensor schematic drawing and corresponding impulse response received from reflector grating. Experimental data – lower trace (red), COM model – upper trace (blue).

thickness also increases with frequency. Therefore, in a device fabricated with a single metal thickness for all reflectors, the magnitude of SAW reflection for each chip will not be equal. The resulting grating responses are shown in Fig. 3.

The OFC SAW transceiver block diagram is shown in Fig. 4. The SAW tag is interrogated with a linear stepped upchirp possessing the same time length and bandwidth as the tag impulse response. For a given peak amplitude, the chirp provides increased power over a given bandwidth as compared to a simple RF tone burst. A noise-like signal is returned from the ID tag as shown on the system block diagram. Since orthogonal frequencies are used, the intersymbol interference is drastically reduced when compared with a conventional PN sequence. A band-limited version of the tag's impulse response results after a down chirp is applied. The signal is then match filtered to produce a compressed pulse.

### IV. OFC SAW SENSOR IMPLEMENTATION

OFC is readily applied to SAW sensing applications. The resulting system offers the advantage of simultaneous sensing and tagging. The sensor is employed by creating identical reflector banks on either side of a wideband transducer as shown in Fig. 5, however, a different free space delay is employed on either side of the device designated by  $\tau_1$  and  $\tau_2$ . The various chip amplitudes caused by the differences in SAW reflection described previously are observed. When this device is used with the transceiver described, two compressed

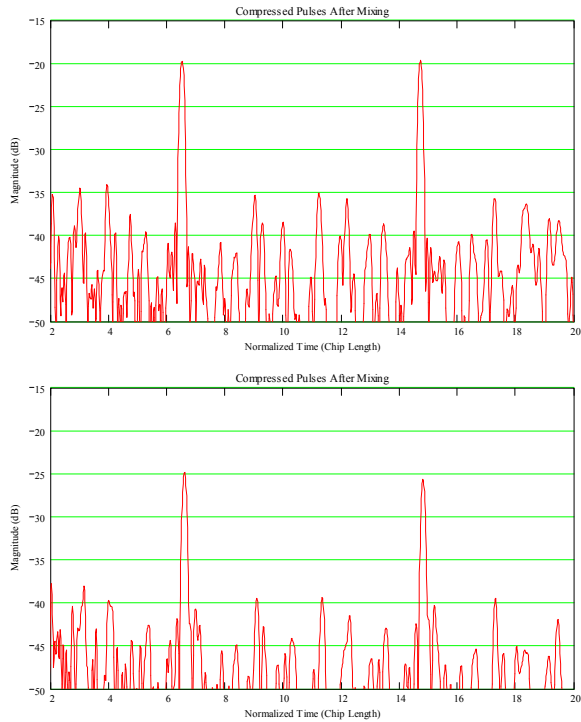


Figure 6. OFC SAW sensor compressed pulses using COM model (above) and experimental device on YZ LiNbO<sub>3</sub> (below).

pulses will result. The differential time delay between pulses gives the sensed information.

The device was simulated using a COM model and verified by experiment using devices fabricated on YZ LiNbO<sub>3</sub>. The designed center frequency was 250 MHz, and seven chips were implemented using seven frequencies which occupied a 25% fractional bandwidth. Each chip was approximately 100 ns long resulting in a bit length of roughly 700 ns. The free space delays,  $\tau_1$  and  $\tau_2$ , were approximately 0.65  $\mu$ s and 1.5  $\mu$ s. The resulting device length was approximately 1 cm. The transceiver was then simulated using the predicted and experimental responses of the sensor. Fig. 6 shows the correlated compressed pulses from the transceiver simulation using the predicted and experimental SAW responses. There is excellent agreement between prediction and experiment. Also note the time ambiguity of the compressed pulses. Each pulse is approximately  $0.28 \cdot \tau_c$  long. This corresponds to a processing gain of 49 which is seven times greater than that of a seven chip PN sequence using a single frequency carrier. As a result, the OFC system has increased range and sensitivity when compared with conventional single frequency pulse implementations.

The device described was tested over temperature to verify temperature sensing capability. The compressed pulse response degraded as temperature was increased as shown in Fig. 7. As the temperature was increased from 12.4°C to 54.1°C the compressed pulse power was decreased by 5 dB and the sidelobe level was increased by 5 dB. This is a direct result of changes in SAW velocity. As velocity changes, errors in the matched filter frequencies, chip lengths, and chip locations increase. In order to compensate for these errors,

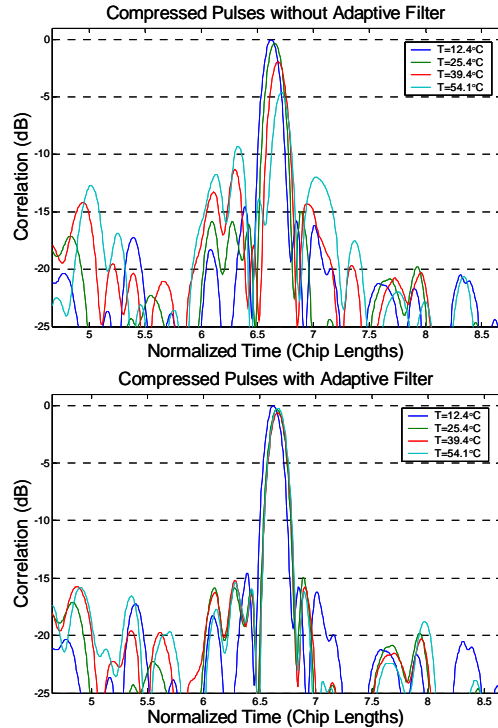


Figure 7. Degradation of compressed pulse response over temperature using static matched filter (upper), and improved compressed pulse response using adaptive matched filter (lower).

previous temperature measurements were used to create an adaptive matched filter with results shown in Fig. 7. The pulse power remains high and the sidelobe level is maintained at -15 dB.

The SAW temperature sensor results are shown in Fig. 8. This plot compares the YZ LiNbO<sub>3</sub> sensor with thermocouple measurements. The measurements were conducted using an RF probe station and a temperature-controlled chuck. The device was tested between 10°C and 180°C in 5°C increments. Overall, there is good agreement between the sensor and thermocouple. It is believed that the errors in the measurements are caused by poor contact to the wafer. Fig. 9 shows the results from the same sensor tested between 15°C and 50°C in 2.5°C increments. This data is shown to be more accurate as the largest error in these measurements was less than 1 C.

## V. CONCLUSION

This paper demonstrated the use of orthogonal frequency coding (OFC) for SAW ID tags and sensors which enables unique sensor operation and identification in multi-sensor environments. A preliminary description of orthogonal frequency coding is given and the OFC technique is applied to SAW ID tags using shorted periodic reflector gratings. A potential transceiver configuration is described and simulated. Inherent advantages to OFC are presented and discussed including reduced time ambiguity of compressed pulses and increased processing gain compared to conventional PN coding using a single carrier frequency. In addition, the

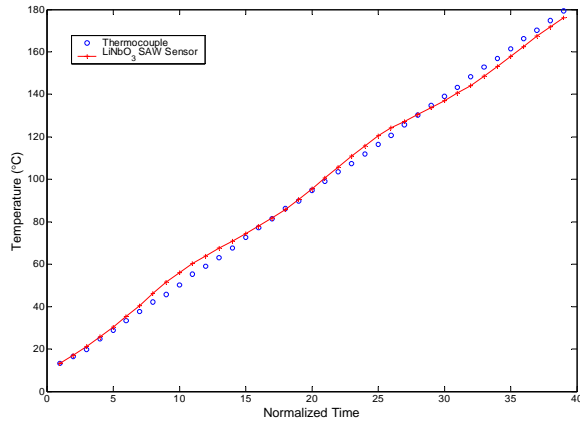


Figure 8. Seven chip OFC SAW temperature sensor tested between 10°C and 180°C and compared to thermocouple measurements

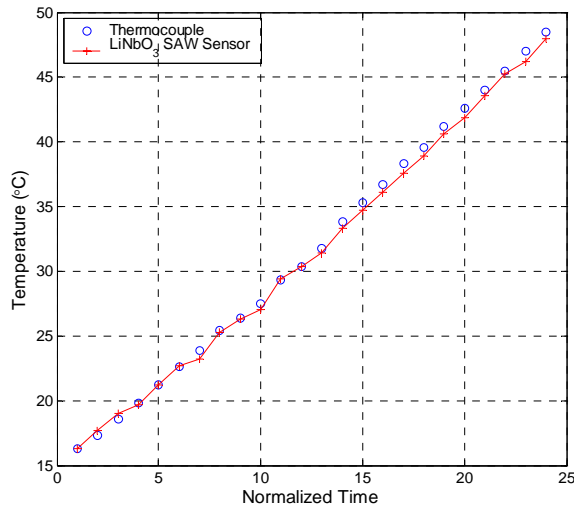


Figure 9. Seven chip OFC SAW temperature sensor tested between 15°C and 50°C and compared to thermocouple measurements

system is inherently secure due to the matched filtering process employed. The techniques employed for SAW ID tags have been extended to create a successful SAW temperature sensor on YZ LiNbO<sub>3</sub>. The sensor was simulated using a COM model and verified by experiment.

#### ACKNOWLEDGMENT

The authors wish to thank NASA for the opportunity to research this work through an STTR program in collaboration with MicroSensor Systems, Inc.

#### REFERENCES

[1] A. Pohl, G. Ostermayer, L. Reindl, and F. Seifert, "Monitoring the tire pressure at cars using passive SAW sensors," 1997 IEEE International Ultrasonics Symposium, pp. 471-474.

[2] E. Benes, M. Gröschl, F. Seifert, and A. Pohl, "Comparison between BAW and SAW sensor principles," IEEE Transactions on Ultrasonics, Ferroelectrics, and Frequency Control, Vol. 45, No. 5, September 1998.

[3] C.S. Hartmann, "A global SAW ID tag with large data capacity," 2002 IEEE International Ultrasonics Symposium, pp. 65-69.

[4] L.L. Yang and L. Hanzo, "Overlapping M-ary frequency shift keying spread spectrum multiple access systems using random signature sequences," IEEE Transactions on Vehicular Technology, Vol. 48, No. 6, pp. 1984-1995, November 1999

[5] S.E. Carter and D.C. Malocha, "SAW device implementation of a weighted stepped chirp code signal for direct sequence spread spectrum communication systems," IEEE Transactions on Ultrasonics, Ferroelectrics, and Frequency Control, Vol. 47, pp. 967-973, July 2000.

[6] D.C. Malocha, D. Puccio, and D. Gallagher, "Orthogonal frequency coding for SAW device applications," 2004 IEEE International Ultrasonics, Ferroelectrics, and Frequency Control 50<sup>th</sup> Anniversary Joint Conference, in press.